Experimental evaluation of changes in strain under compressive fatigue loading of brick masonry

I.S. Koltsida[a,1], A.K. Tomor[a], C.A. Booth[a]

[a] Faculty of Environment and Technology, University of the West of England, Frenchay Campus, Coldharbour Lane, Bristol BS16 1QY, UK

[1] Corresponding author. Tel.: +44 (0) 1173283049. E-mail addresses: Iris.Koltsida@uwe.ac.uk.

ABSTRACT

Assessing the long-term performance of masonry structures and their response to increased loading conditions are critical to safety and maintenance. A series of laboratory tests have been carried out on brick masonry to assess its performance under long-term fatigue loading. The relationship between stress levels and number of cycles to failure was identified under compressive loading, together with stress-strain evolution at various stress levels. Strain evolution shows distinctive characteristics for the three stages of deterioration and increased strain for increased number of cycles. Experimental results provide useful data for developing analytical prediction models for the fatigue deterioration of masonry structures.

Keywords: Brick Masonry, Fatigue, Strain Evolution, Stress-Strain curves, SN curves

---

1. Introduction

The longest standing bridges around the world are masonry arch bridges, representing around 40% of the highway, railway and waterway bridge infrastructure in Europe [1]. Due to their age and constantly increasing weight, speed and density of traffic, their assessment and maintenance are becoming increasingly important to ensure their continued safe performance.

High-cycle fatigue loading experienced over 100+ years of service life can lead to significant changes on the material level and deterioration below serviceability or ultimate failure load [2]. Identifying the rate of fatigue deterioration and changes in the material properties for masonry are necessary to enable improved assessment of load capacity, remaining service life, optimising traffic loading and planning maintenance works.

Limited data is however available for assessing the fatigue capacity of masonry structures. Some experimental data is available on SN curves (stress vs. number of cycles) for masonry under fatigue loading (Abrams *et al.*, 1985; Clark, 1994; Ronca *et al.* 2004; Roberts *et al.*, 2006; Tomor & Verstrynge, 2013; Tomor *et al.*, 2013) but minimal information has been presented on the evolution of strain under fatigue deterioration.

Abrams *et al.* [3] performed experimental test series on brickwork prisms to investigate the mechanics of masonry under cyclic compressive stress. Abrams *et al.* concluded that cyclic loading leads to gradual reduction in the compressive strength of masonry and that the rate of reduction is a function of the mortar strength, amplitude and number of cycles. Greater cyclic stress levels and stronger mortars accelerate deterioration. Clark [4] conducted similar experiments and proposed SN curves for dry and wet masonry, suggesting a fatigue limit for dry brick masonry around ~50% of its quasi-static compressive strength.

Roberts *et al.* [5] defined a lower bound fatigue strength for dry, submerged and wet brick masonry based on a series of quasi-static and high cycle fatigue tests on brick masonry (Equation 1.1).

$$F(S) = \frac{(\Delta\sigma\sigma_{max})^{0.5}}{f_c} = 0.7 - 0.05\, log\, N \quad 1.1$$

Where F(S) is the function of the induced stress, $\Delta\sigma$ is the stress range, σ_{max} is the maximum stress, f_c is the quasi-static compressive strength of masonry and N is the number of load cycles.

Casas [2] proposed a probability-based fatigue model for brick masonry under compression with different defined confidence levels based on the experimental data reported by Roberts *et al.* [5] (Equation 1.2).

$$S_{max} = A \times N^{-B(1-R)} \qquad 1.2$$

Where S_{max} is the ratio of the maximum loading stress to the quasi-static compressive strength, N is the number of cycles to failure and R is the ratio of the minimum stress to the maximum stress $\sigma_{min}/\sigma_{max}$. Coefficients A and B depend on the value of the survival function and were calculated by Casas [2].

Tomor and Verstrynge [6] proposed a joined fatigue-creep deterioration model. A probabilistic fatigue model was suggested by adapting Casas' [7] model and introducing a correction factor C, allowing the interaction between the creep and fatigue phenomena to be taken into account and adjusting the slope of the SN curve (Equation 1.3).

$$S_{max} = A \cdot N^{-B(1-C \cdot R)} \qquad 1.3$$

Where S_{max} is the ratio of the maximum stress to the average compressive strength ($S_{max} = \sigma_{Max}/f_c$), N the number of cycles, R the ratio of the minimum stress to the maximum stress ($R = \sigma_{Min}/\sigma_{Max}$), parameter A is set to 1, parameter B is set to 0.04 and C is the correction factor.

Tomor and Verstrynge [6] identified three stages of fatigue deterioration with the use of an acoustic emission technique to monitor the response of masonry prisms under long-term fatigue in compression. During the first stage (0-75% of the total number of cycles), the acoustic emission levels were relatively low and constant. A small increase in emission was observed in the second stage (75-95% cycles), followed by rapid increase in emission and sudden failure during the third stage (95-100% cycles).

Tomor *et al.* [8] also identified three distinct stages of fatigue deterioration based on acoustic emission levels. During Stage I, reduction in emission was observed (0-32% of the total loading cycles for compression and 0-58% for shear). During Stage II, emission stabilised (32-67% for compression, not evident in shear) and in Stage III rapid increase in emission was observed, leading to failure (67-100% for compression, 58-100% shear).

Carpinteri *et al.* [9] performed a series of quasi-static and cyclic tests (8 specimens tested at 70%

stress) on brick masonry specimens and walls and suggested a ε-N curve (strain vs. number of cycles) with three distinctive stages. During Stage I deformations increased rapidly for the first 10% of loading cycles, during Stage II deformations increased at a constant rate (10-80% of loading cycles) and during Stage III deformations increased rapidly again, leading to failure. Carpinteri *et al.* [9] also related the rate of change in vertical deformation during Stage II ($\vartheta\varepsilon_v/\vartheta n$) to the number of cycles at failure (N_f cycles) as shown in Equation 1.4.

$$N_f = a\left(\frac{\vartheta\varepsilon_v}{\vartheta n}\right)^b \qquad 1.4$$

Where ε_v is the vertical deformation, n is the number of cycles and N_f is the number of loading cycles at failure. Parameters *a* and *b* are material constants, that can be evaluated experimentally by applying a number of loading cycles on a prism up to the point here deformation starts to increase at a constant rate (over 10% of the fatigue life).

There are conflicting results for the different stages of fatigue for masonry and a lack of experimental data for identifying appropriate SN curves for different types of masonry and the evolution of strain under fatigue loading. The aim of this study is to i) investigate the stages of fatigue deterioration, ii) investigate the evolution of strain and stress-strain curves and iii) provide test data to develop mathematical models to predict the fatigue life of masonry.

2. Quasi-static and long-term cyclic tests under compression

Based on the work of Roberts *et al.* [5] and Tomor *et al.* [8], a series of brick masonry prisms have been tested under quasi-static and long-term cyclic compressive loading to identify changes in the material properties of masonry.

2.1 Materials

The experimental study intends to represent the weakest form of masonry, widely found in the UK waterways network, originating from the 1750s-1850s. Brick masonry prisms were built using handmade low-strength solid 210x100x65 mm^3 Michelmersh bricks (B1 bricks). The average compressive strength of the bricks was 4.86 N/mm^2 (1.19 N/mm^2 standard deviation (SD) and 24.48% coefficient of variation) and the gross dry density 1823 kg/m^3. Lime-mortar with 0:1:2 cement: lime: sand by volume (M01 mortar) was used with

NHL3.5 lime and 3 mm sharp washed sand and the mortar joins were 8 mm thick.

2.2 Test specimens

Small-scale masonry prisms (B1M01) comprised of five stack-bonded bricks with four 8 mm mortar joints built according to the ASTM standards (ASTM, 2014) with total dimensions of 210 x 100 x 357 mm^3 (Figure 2-1). In order to have systematic building quality, the same experienced master stonemason constructed all specimens.

Specimens were cured at room temperature for a minimum of five days, stored outdoors for a maximum of six months and acclimatised for a minimum of three days at room temperature prior to testing (Oliveira *et al*., 2006).

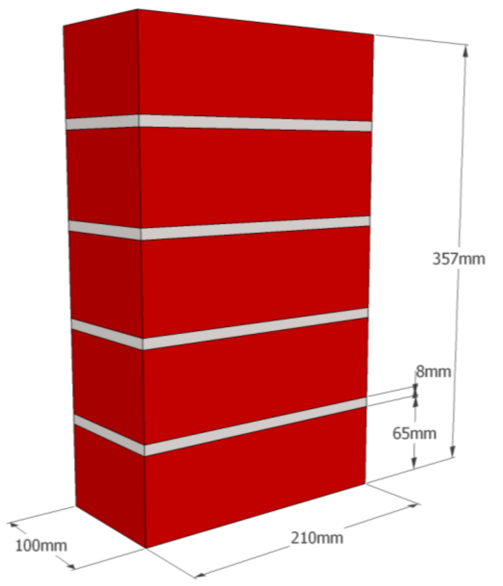

Figure 2-1 Masonry prism dimensions

2.3 Test setup, preparation and instrumentation

Specimens were tested under compression using a 250 kN actuator. Deflections were monitored using four Linear Variable Differential Transformers (LVDTs) with ±5 mm linear range and 0.07% accuracy. Two LVDTs were attached at the front and two in the back of the prisms (Figure 2-2). LVDTs were positioned at 10 mm distance from the edges of the prisms and set against wooden blocks (Tomor & Verstrynge, 2013; Tomor *et al.*, 2013). The distance between the wooden blocks and the LVDTs was ca. 81 mm and included two mortar joints (8 mm each) and one brick (65 mm).

The upper and lower surfaces of the prisms were brushed to remove loose particles and ground flat prior to the test (Oliveira *et al.*, 2006; ASTM, 2014). Prisms were placed, subsequently, between layers of 3 mm plywood and 30 mm steel plates to ensure effective load distribution and to reduce localised stress concentrations (Tomor & Verstrynge, 2013; Tomor *et al.*, 2013).

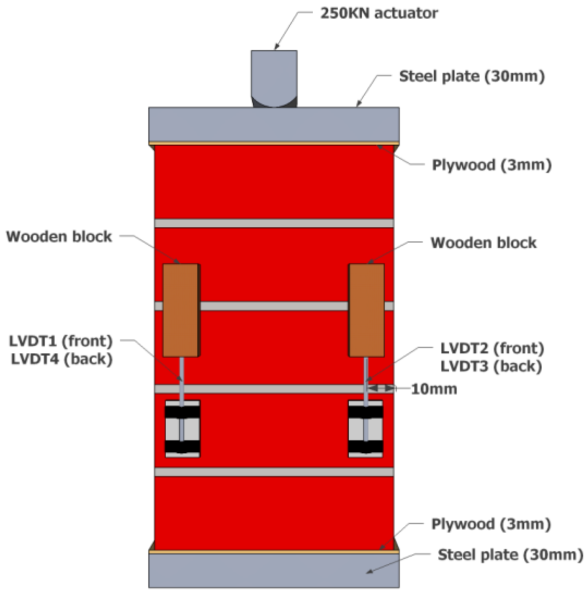

Figure 2-2 Instrumentation of prisms

2.4 Loading

Three sets of tests were performed under quasi-static and fatigue loading to identify material properties and to investigate changes in the material during high-cycle compressive fatigue loading of masonry prisms.

- <u>Quasi-Static tests.</u> A set of six prisms were tested under displacement-controlled quasi-static compression to obtain the mean compressive strength of the material. Loading was applied at 0.01 mm/sec rate of displacement to obtain the full stress-strain curve.
- <u>Fatigue tests - Type I.</u> Masonry prisms were tested under long-term compressive cyclic loading at 2 Hz frequency to identify the number of cycles to failure at different stress levels. Before the start of the fatigue tests, quasi-static loading was applied up to the mean fatigue load. Fatigue loading was subsequently applied in a sinusoidal pattern (Figure 2-3), between defined minimum and maximum stress levels.

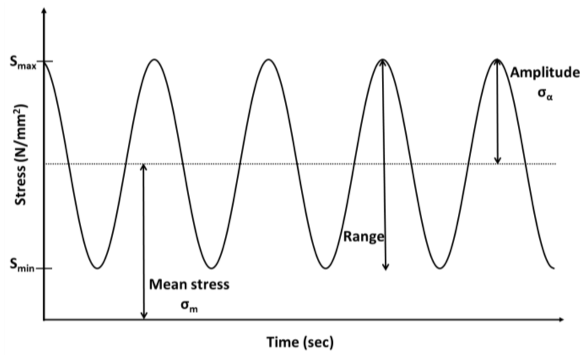

Figure 2-3 Sinusoidal load pattern for Type I fatigue tests

The minimum (Smin) and maximum (Smax) stress levels were expressed as percentage of the mean ultimate quasi-static strength. The minimum stress represent the dead load of the structure due to its self-weight and was set to 10% of the ultimate compressive strength to enable the most extreme range of fatigue loading to be applied.

The maximum stress level represents live load (e.g. similar to traffic over a masonry arch bridge) and ranged between 55% and 80% (55%, 60%, 68%, 80%) of the ultimate compressive strength for the individual specimens.

- Fatigue tests - Type II. The second set of fatigue tests was designed to identify stages during fatigue deterioration and evolution of the stress-strain curves. Loading was first applied statically up to the mean fatigue stress level σ_m under displacement control at a 0.01 mm/sec loading rate (Branch A, Figure 2-4), cycled sinusoidally between the minimum and maximum load levels for 1000 cycles (Branch B, Figure 2-4) and unloaded (Branch C, Figure 2-4). The process was repeated until failure occurred. Branch A was used to identify the stress-strain relationship, up to the mean fatigue stress level, every 1000 cycles during the fatigue life of the prisms. Similarly to Type I fatigue tests, the minimum stress level was set to 10% of the compressive strength and the maximum stress level was set to 63%, 68% and 73% for the individual specimens.

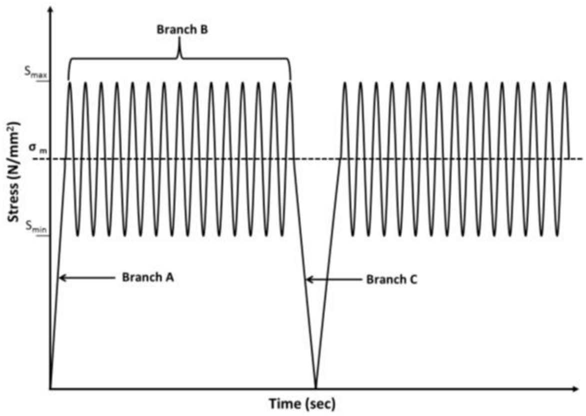

Figure 2-4 Load pattern for Type II fatigue tests (Branch A quasi-static loading, Branch B cyclic loading, Branch C unloading)

3. Results

3.1 Quasi-static tests

The mean compressive strength for the set of B1M01 prisms tested, according to BS EN 1052-1:1999, was 2.94 N/mm^2 (SD 0.10 N/mm^2). During quasi-static compression vertical cracks developed initially around the middle of the specimens and subsequently on the narrow sides, leading to failure (Figure 3-1).

3.2 Fatigue Tests – Type I.

A total of 32 prisms were tested to failure under maximum stress levels of 55, 60, 68 or 80% of the average quasi-static compressive strength (see section 2.4). The maximum number of loading cycles was recorded and shown in Table 3-1.

Table 3-1 Fatigue test results - Type I

Specimen Name	Load range (kN)	Stress Range (N/mm^2)	N	Specimen Name	Load range (kN)	Stress Range (N/mm^2)	N
B1M01-18	6-49	0.29-2.33	2,566	B1M01-57	6-42	0.29-2.00	1,100
B1M01-48	6-49	0.29-2.33	14,073	B1M01-26	6-37	0.29-1.76	25,342
B1M01-49	6-49	0.29-2.33	2,832	B1M01-28	6-37	0.29-1.76	2,646,302
B1M01-50	6-49	0.29-2.33	456	B1M01-29	6-37	0.29-1.76	122,762
B1M01-19	6-42	0.29-2.00	1,800	B1M01-30	6-37	0.29-1.76	1,268,627
B1M01-20	6-42	0.29-2.00	3,600	B1M01-31	6-37	0.29-1.76	3,528,118
B1M01-21	6-42	0.29-2.00	13,000	B1M01-32	6-37	0.29-1.76	986,325
B1M01-22	6-42	0.29-2.00	17,350	B1M01-33	6-37	0.29-1.76	796,744
B1M01-23	6-42	0.29-2.00	18,651	B1M01-34	6-34	0.29-1.62	56,562
B1M01-24	6-42	0.29-2.00	18,276	B1M01-40	6-34	0.29-1.62	412,774
B1M01-35	6-42	0.29-2.00	3,000	B1M01-41	6-34	0.29-1.62	1,088,560
B1M01-36	6-42	0.29-2.00	6,737	B1M01-43	6-34	0.29-1.62	2,200
B1M01-53	6-42	0.29-2.00	134	B1M01-44	6-34	0.29-1.62	4,864
B1M01-54	6-42	0.29-2.00	3,541	B1M01-45*	6-34	0.29-1.62	10,225,676
B1M01-55	6-42	0.29-2.00	5,994	B1M01-46	6-34	0.29-1.62	1,724,587
B1M01-56	6-42	0.29-2.00	212	B1M01-47	6-34	0.29-1.62	1,672,237
* No failure, testing discontinued							

The failure patterns under fatigue loading were very similar to quasi-static loading with vertical splitting cracks along the middle of the specimens, leading to failure (Figure 3-1).

Results of the quasi-static and fatigue compression tests are shown in Figure 3-2 together with proposed SN relationships by Casas [2] and Tomor & Verstrynge [6]. Quasi-static test results are included as failure at 1 cycle. The SN relationship by Casas [2] gives a good indication of the mean number of cycles at each stress level, while the relationship by Tomor and Verstrynge [6] incorporates the quasi-static test results, although slightly overestimates the mean number of cycles.

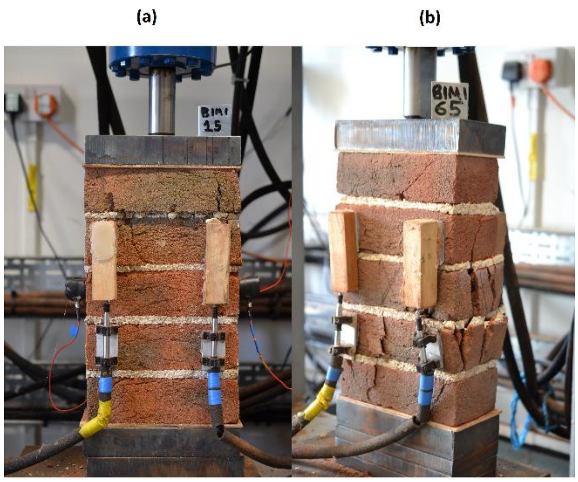

Figure 3-1 Typical failure pattern under (a) quasi-static compression and (b) fatigue compression

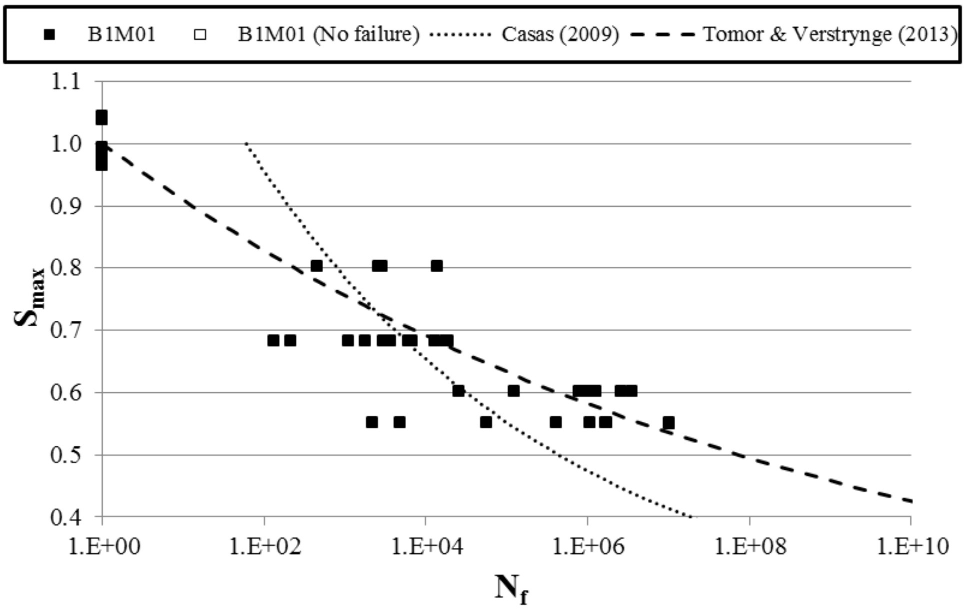

Figure 3-2 Fatigue test data together with SN curves [2, 6].

During the Type I Fatigue tests, maximum and minimum total longitudinal displacements were recorded and the strain evolution curves (ε-N/N_f) plotted for each stress level in Figure 3-3 to Figure 3-6 (for 55, 60, 68, 80% maximum stress respectively). The ε-N curves exhibit a typical S shape (Holmen, 1982; Carpinteri *et al.*, 2014), with three distinct stages:

Stage I: rapid increase of strain during the first 10% of the life expectancy, caused by initiation of micro-cracks.

Stage II: reveals a gradual increase of strain for approximately 80% of the total number of cycles, caused by development of micro-cracks.

Stage III: rapid increase of strain during the last 10-20% of life expectancy, caused by coalition of micro-cracks into macro-cracks and leading to failure.

Carpinteri *et al*. [9] indicated that Stage II lasts until 80% of the fatigue life of masonry based on limited tests under 70% stress, while according to the data presented here, Stage II occupies the range between 10% and 90% of the total loading cycles sustained by a prism at different stress levels. Carpinteri *et al*. [9] proposed the use of equation 1.4 to correlate the vertical deformation with the number of cycles. The strain evolution could be more precisely described by three distinct equations (parabolic type for stage I and Stage III and linear type for stage II) for the different fatigue stages that would consider the effect of stress level.

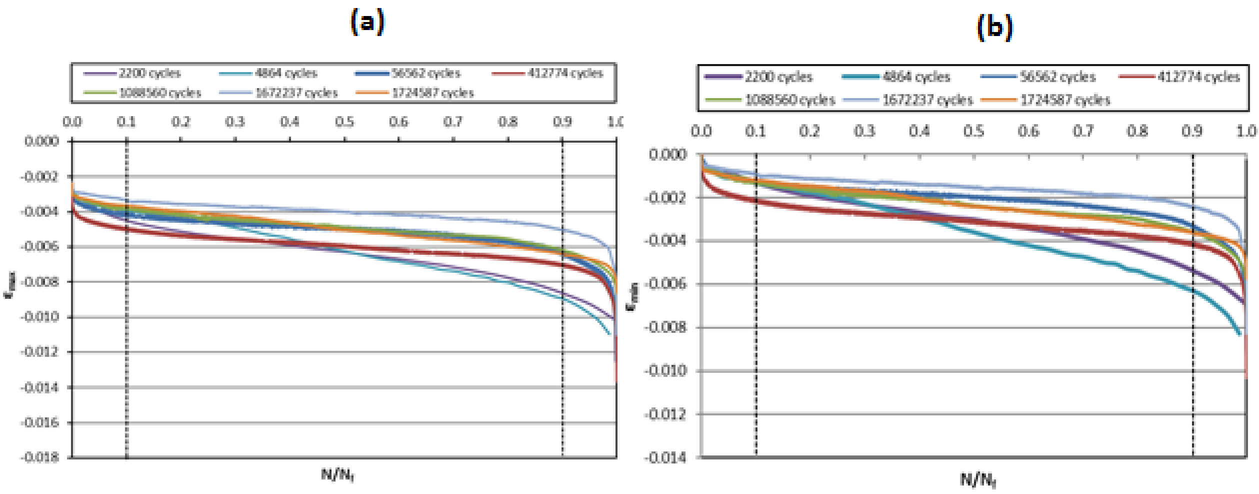

Figure 3-3 Total longitudinal strain variation with the cycle ratio for 55% maximum stress level (a) maximum total strain, (b) minimum total strain

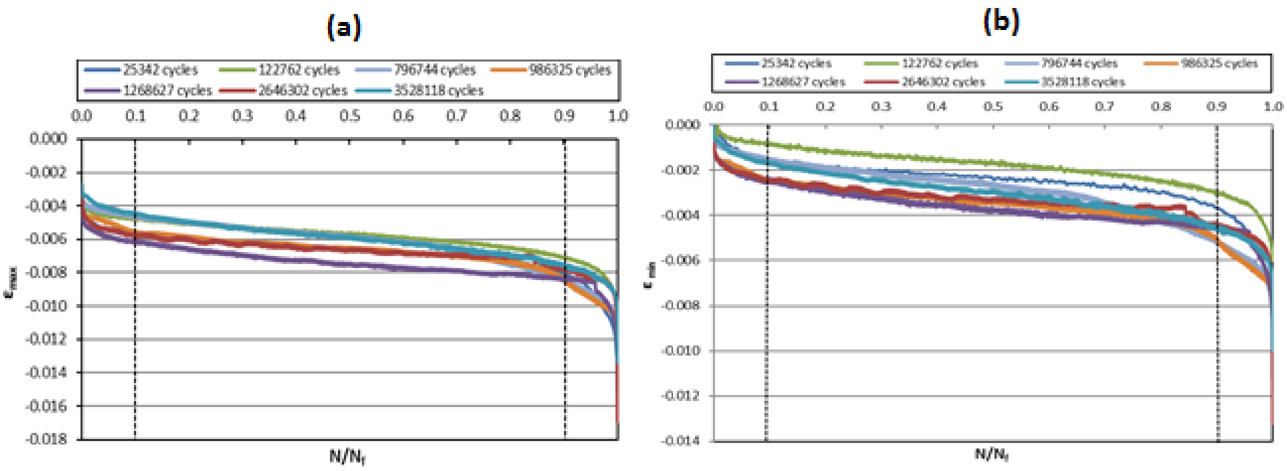

Figure 3-4 Total longitudinal strain variation with the cycle ratio for 60% maximum stress level (a) maximum total strain, (b) minimum total strain

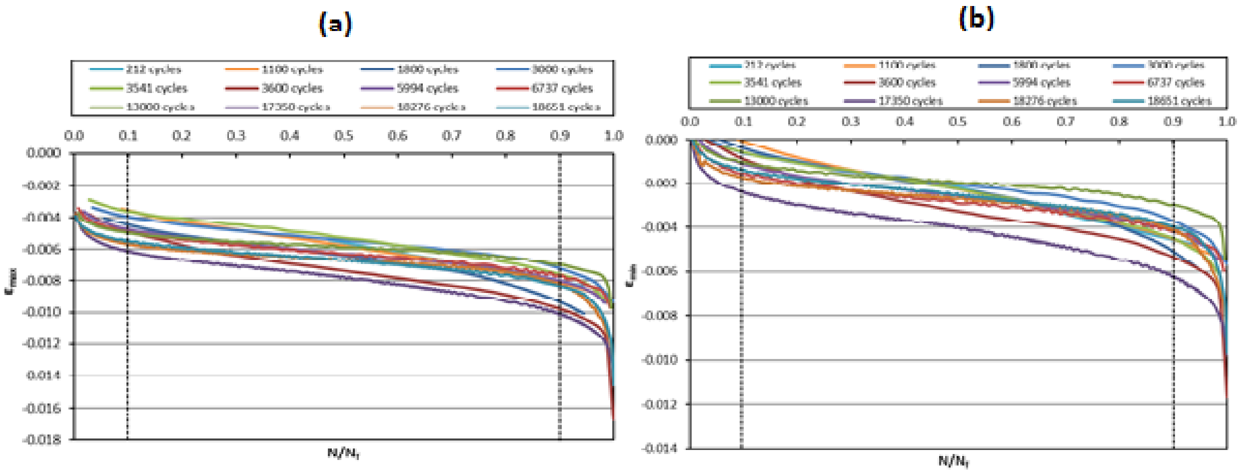

Figure 3-5 Total longitudinal strain variation with the cycle ratio for 68% maximum stress level (a) maximum total strain, (b) minimum total strain

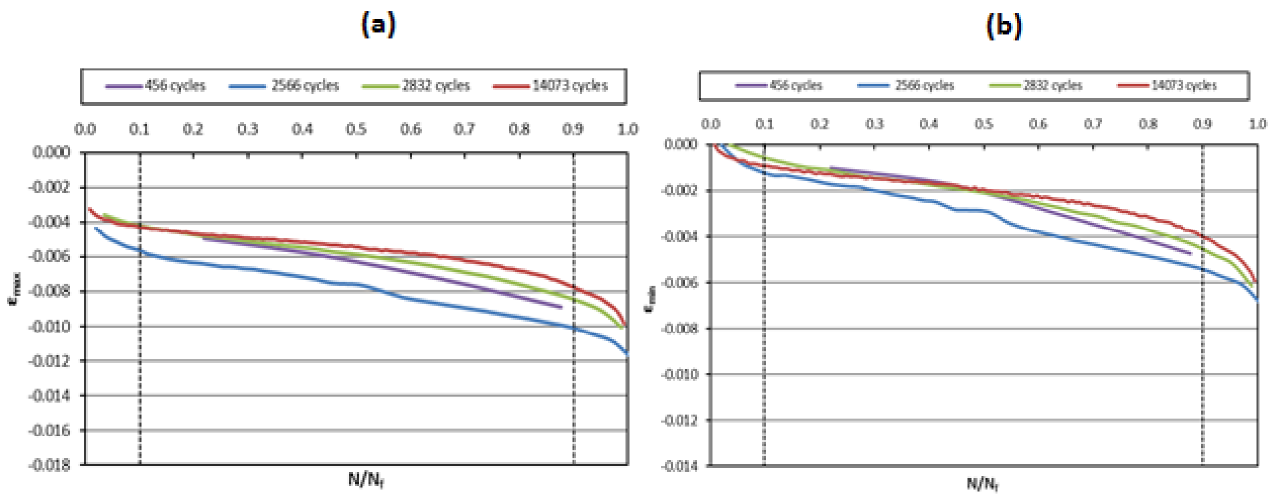

Figure 3-6 Total longitudinal strain variation with the cycle ratio for 80% maximum stress level (a) maximum total strain, (b) minimum total strain

Three stages of strain development have already been identified in concrete under fatigue loading (Holmen, 1982; Kim & Kim, 1996; Breitenbucher & Ibuk, 2006; Zanuy *et al.*, 2011) and also for masonry (Carpinteri *et al.*, 2014).

The rate of strain evolution at Stage II is noticeably steeper for higher stress levels (as shown in Figure 3-7 for maximum stress levels 55%, 60%, 68% and 80%). This indicates a faster rate of the fatigue process at higher stress levels leading to earlier failure of the specimen.

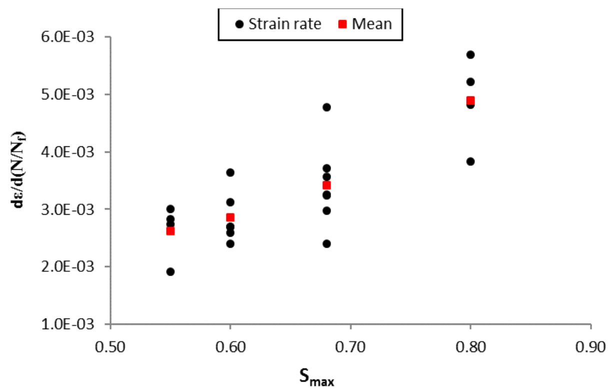

Figure 3-7 Strain rate ($d\varepsilon/d(N/N_f)$) for 55%, 60%, 68%, 80% maximum stress during Stage II Fatigue test - Type I

3.3 Fatigue tests – Type II

Masonry prisms were tested under 73%, 68% and 63% maximum compressive stress during Type II fatigue tests (see Section 2.4) and results listed in Table 3-2 to Table 3-4.

Table 3-2 Fatigue test results - Type II, 73% maximum stress

Specimen Name	Load Range (kN)	Stress Range (N/mm^2)	N
B1M01-66	6-45	0.29-2.14	253
B1M01-67	6-45	0.29-2.14	200
B1M01-68	6-45	0.29-2.14	413
B1M01-69	6-45	0.29-2.14	53
B1M01-70	6-45	0.29-2.14	55
B1M01-76	6-45	0.29-2.14	7
B1M01-77	6-45	0.29-2.14	104
B1M01-78	6-45	0.29-2.14	240
B1M01-85	6-45	0.29-2.14	93

Table 3-3 Fatigue test results - Type II, 68% maximum stress

Specimen Name	Load Range (kN)	Stress Range (N/mm^2)	N
B1M01-58	6-42	0.29-2.00	31,000
B1M01-59	6-42	0.29-2.00	69,537
B1M01-60	6-42	0.29-2.00	34
B1M01-61	6-42	0.29-2.00	71,342
B1M01-62	6-42	0.29-2.00	11,754
B1M01-63	6-42	0.29-2.00	37,938
B1M01-64	6-42	0.29-2.00	33,752
B1M01-65	6-42	0.29-2.00	275,000

Table 3-4 Fatigue test results - Type II, 63% maximum stress

Specimen Name	Load Range (kN)	Stress Range (N/mm^2)	Number of cycles
B1M01-71	6-39	0.29-1.86	718
B1M01-72	6-39	0.29-1.86	11,038
B1M01-73	6-39	0.29-1.86	269
B1M01-74	6-39	0.29-1.86	2,515
B1M01-75	6-39	0.29-1.86	1,104
B1M01-79	6-39	0.29-1.86	266
B1M01-80	6-39	0.29-1.86	19,203
B1M01-81	6-39	0.29-1.86	54
B1M01-82	6-39	0.29-1.86	34,728
B1M01-83	6-39	0.29-1.86	3,355
B1M01-84	6-39	0.29-1.86	256
B1M01-86	6-39	0.29-1.86	59,921
B1M01-87	6-39	0.29-1.86	543
B1M01-88	6-39	0.29-1.86	4,809
B1M01-89	6-39	0.29-1.86	881

Evolution of the stress-strain curves for 68% and 63% maximum stress identified every 1000 cycles (every 500 cycles for B1M01-83 and B1M01-88) are shown in Figure 3-8 and Figure 3-9. No stress-strain curve could be identified for 73% stress due to rapid deterioration and failure under 300 cycles. The stress-strain curve is straight initially (or slightly concave towards the strain axis) and becomes convex and increasingly curved for increasing load cycles. The residual strain is large in Stage I, decreases and stabilises in Stage II and increases fast again in Stage III. Concrete exhibits similar behaviour under fatigue loading [10, 11].

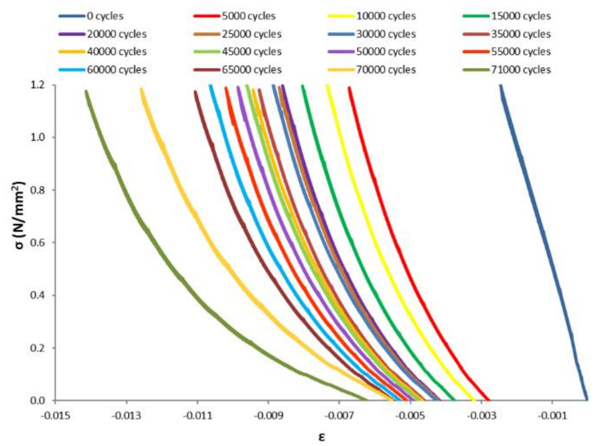

Figure 3-8 Stress-strain curve development every 1000 cycles under 68% maximum stress (B1M01-61)

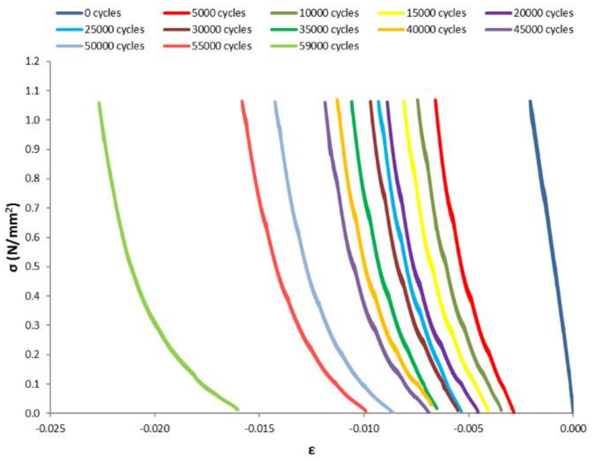

Figure 3-9 Stress-Strain curve development every 1000 cycles under 63% maximum stress *(B1M01-86)*

It is noteworthy that the maximum recorded strains at failure, during quasi-static compressive tests are noticeably lower compared to respective strains under fatigue loading. Thus, prior cyclic loading of a masonry prism imposes additional deformation.

The maximum strain at failure is the lowest under quasi-static loading (0.002-0.005; mean 0.003; SD 0.001) and increases for lower fatigue stress levels (0.005-0.018; mean 0.012; SD 0.005 for 68% maximum stress and 0.017-0.025; mean 0.020; SD 0.003 for 63% maximum stress). Increased strain under lower fatigue stress levels is likely to be associated with increasing effect of creep. For extended test durations creep damage is accumulated during the relatively longer time spent near the peak stress of each cycle.

4. Discussion

Masonry arch bridges are subjected to increasing traffic loading and gradual material deterioration due to environmental impact and fatigue loading. Changes in the material properties have direct influence on the load carrying capacity and rate of deterioration of the overall structure. Very little guidance is, however, available for estimating changes in the material properties for masonry over time. Test data will next be used to develop mathematical models for the evolution of material properties under fatigue compressive loading. Mathematical models can in turn be used for improved modelling of masonry under changing load regimes and estimating the load-carrying capacity over time to improve assessment, maintenance and restoration masonry arch bridges.

The fatigue life of the structure can be evaluated by available SN models [2, 6]. Past and future loading history may be estimated using simplified load models, e.g. Miner's Rule (Equation 4.1) [12] to evaluate the residual service life.

$$\frac{n_1}{N_1} + \cdots + \frac{n_{i-1}}{N_{i-1}} + \frac{n_i}{N_i} < 1 \qquad 4.1$$

Where ni is the number of cycles at any stress range and Ni is the number of cycles causing failure at the corresponding stress range. Knowing the number of cycles that the structure has experienced an appropriate stress-strain curve can be selected for the assessment of a masonry arch bridge (e.g. using finite element models).

Changes in the deformability of a masonry arc bridge under traffic loading, observed during monitoring, can be associated with the experimentally recorded ε-N curve configuration and contribute to appropriate maintenance planning. The configuration of the ε-N curve indicates that strain changes with high rate and in parabolic shape during stage I and III and linearly at a constant rate during the second stage. An observed sudden change during long-term monitoring of a structure from linear growth of strain to a non-linear trend could mean that the structure is undergoing stage III and major strengthening is required or traffic needs to be diverted.

5. Conclusions

This study presents test results from small-scale laboratory tests on changes of the material properties of masonry under compressive fatigue loading.

Strain evolution curves (ε-N) exhibit a typical 'S' configuration with three distinct stages. During the first stage (10% of N_f), strains grow rapidly indicating initiation of micro-cracks. Stage II is the dominant stage (10-90% of N_f) during which the strains grow steadily until Stage III (90-100% of N_f), at which point, coalition of micro-cracks to macro-cracks leads to sudden failure of the prism. The rate of strain evolution in Stage II of the fatigue life is lower for lower stress levels.

The configuration of the stress-strain curve changes during cyclic compressive loading from concave with respect to the strain axis to convex with greater curvature for increased loading cycles. Large initial change in the residual strain is observed in Stage I, reduced and relatively constant strain in Stage II and increases again in Stage III.

Prior cyclic loading of masonry imposes additional deformation. The maximum strain at failure is greater for lower fatigue stress levels, likely to be due to the effect of creep for longer test durations.

Test data will be used to develop probability based mathematical models for the evolution of material properties under fatigue compressive loading. Improved models for material properties will enable enhanced modelling of masonry arch bridges and estimation of the load carrying capacity and remaining service life over time.

Acknowledgement

The work reported in this paper was supported by the International Union of Railways (UIC). The technical and financial support provided, is gratefully acknowledged by the authors.

References

[1] S. Sustainable Bridges Project, "European Railway Bridge Demography, Deliverable D1.2 – Technical report," 2004.

[2] J. R. Casas, "A probabilistic fatigue strength model for brick masonry under compression," *Construction and Building Materials*, vol. 23, no. 8, pp. 2964-2972, 2009.

[3] D. P. Abrams, J. L. Noland and R. H. Atkinson, "Response of Clay-unit Masonry to Repeated Compressive Forces," Melbourne, Australia, 1985.

[4] G. Clark, "Bridge Analysis Testing and Cost Causation Project: Serviceability of Brick

Masonry," British Rail Research Report No. LR-CES-151, 1994.

[5] T. Roberts, T. Hughes, V. Dandamudi and B. Bell, "Quasi-static and high cycle fatigue strength of brick masonry," *Construction and Building Materials*, vol. 20, no. 9, pp. 603-614, 2006.

[6] A. Tomor and E. Verstrynge, "A joint fatigue–creep deterioration model for masonry with acoustic emission based damage assessment," *Construction and Building Materials*, vol. 43, no. 1, pp. 575-588, 2013.

[7] J. R. Casas, "Reliability-based assessment of masonry arch bridges," *Construction and Building Materials*, vol. 25, no. 4, pp. 1621-1631, 2011.

[8] A. Tomor, S. De Santis and J. Wang, "Fatigue deterioration process of brick masonry," *Journal of the International Masonry Society*, vol. 26, no. 2, pp. 41-48, 2013.

[9] A. Carpinteri, A. Grazzini, G. Lacidogna and A. Manuello, "Durability evaluation of reinforced masonry by fatigue tests and acoustic emission technique," *Structural Control and Health Monitoring*, vol. 21, no. 6, pp. 950-961, 2014.

[10] J. Crumley and W. Kennedy, "Fatigue and Repeated-load Elastic Characteristics of Inservice Portland Cement Concrete," Center of highway research, The University of Texas, Texas, USA, 1977.

[11] J. O. Holmen, "Fatigue of concrete by constant and variable amplitude loading," *ACI*, vol. 75, no. 0, pp. 71-110, 1982.

[12] M. Miner, "Cumulative damage in fatigue," *Journal of Applied Mechanics*, vol. 67, pp. A159-A164, 1945.

[13] D. V. Oliveira, P. B. Lourenço and P. Roca, "Cyclic behaviour of stone and brick masonry under uniaxial compressive loading," *Materials and Structures*, vol. 39, no. 2, pp. 247-257, 2006.

[14] P. Ronca, A. Franchi and P. Crespi, "Structural failure of historic buildings: masonry fatigue tests for an interpretation model," *Structural Analysis of Historical Constructions*, vol. 2, no. 1, pp. 273-279, 2004.

[15] C. Zanuy, L. Albajar and P. de la Fuente, "The fatigue process of concrete and its structural influence," *Materiales de Construccion*, vol. 61, no. 303, pp. 385-399, 2011.

[16] ASTM, "Standard test method for compressive strength of masonry prisms," in *Annual Book of ASTM Standards*, vol. 4.05, ASTM, Ed., West Conhohocken, ASTM International, 2014, pp. 889-895.

[17] R. Breitenbucher and H. Ibuk, "Experimentally based investigations on the degradation-process of concrete under cyclic loading," *Materials and Structures*, vol. 39, no. 7, pp. 717-724, 2006.

[18] J. Kim and Y. Kim, "Experimental study of the fatigue behavior of high strength concrete," *Cement and Concrete Research*, vol. 26, no. 10, pp. 1513-1523, 1996.